Tikrit Journal of Engineering Sciences (2024); 31(3): 93-104
DOI: http://doi.org/10.25130/tjes.31.3.9

IRAQI Academic Scientific Journals

ISSN: 1813-162X (Print); 2312-7589 (Online)

Tikrit Journal of Engineering Sciences

available online at: http://www.tj-es.com

TJES Tikrit Journal of Engineering Sciences

Evaluating the Hydraulic Performance of USBR II Stilling Basin with Rough Bed

Layla A. M. Saleh *, **Saleh I. Khassaf**
Civil Department, Engineering College, Basrah University, Basrah, Iraq.

Keywords:
Hydraulic jump; Numerical simulation; Relative energy dissipation; Roughness; Sequent depth ratio; Stilling basin.

Highlights:

- *USBR II stilling basin with rough bed, downstream an ogee spillway, as a modified energy dissipation structure.*
- *Numerical modeling was performed utilizing Flow-3D program.*
- *The modified basin outperformed the typified basin.*

ARTICLE INFO
Article history:

Received	12 Sep.	2023
Received in revised form	12 Oct.	2023
Accepted	19 Oct.	2023
Final Proofreading	08 Jan.	2024
Available online	17 July	2024

Citation: Saleh LAM, Khassaf SI. **Evaluating the Hydraulic Performance of USBR II Stilling Basin with Rough Bed**. *Tikrit Journal of Engineering Sciences* 2024; **31**(3): 93-104.
http://doi.org/10.25130/tjes.31.3.9

Corresponding author:

Layla A. M. Saleh
Civil Department, Engineering College, Basrah University, Basrah, Iraq.

Abstract: Stilling basins are built in conjunction with dams, weirs, and gates to dissipate the high kinetic energy of incoming flow and prevent severe scouring of the downstream riverbed. Dissipation of this high energy can be achieved through forming a hydraulic jump. The hydraulic jump features, including the relative length, ratio of sequent depth, and energy dissipation, are utilized as criteria to evaluate the efficiency of the stilling basin operation. The present study involved conducting experimental and numerical tests to evaluate the performance of the USBR II stilling basin downstream of an ogee spillway using six upstream Froude numbers ranging between 6.37 and 14.97. Experiments were conducted for the Typified USBR II stilling basin. The results were used to perform mesh sensitivity for numerical simulation. The USBRII stilling basin with different rough beds was numerically simulated using FLOW-3D software. The rough beds were designed using three roughness intensities, 10%, 15%, and 22%, and three relative roughness heights: 1, 0.75. and 1. According to the numerical results, distributing staggered cubic elements in the bed of the USBR II stilling basin at 10% intensity and a relative roughness height of (1) enhanced the stilling basin performance compared to the smooth bed and other rough beds. In the case of the best roughness bed, the sequent depth ratio decreased by about 12.1%, and the energy dissipation enhanced by around 5.1% compared to the Typified basin.

تقييم الأداء الهيدروليكي لأحواض التهدئة ذات الأرضية الخشنة

ليلى علي محمد صالح، صالح عيسى خصاف
قسم الهندسة المدنية/ كلية الهندسة / جامعة البصرة / البصرة – العراق.

الخلاصة
يتم بناء أحواض التهدئة جنبًا إلى جنب مع السدود والهدارات والبوابات لتشتيت الطاقة الحركية العالية لتدفق الماء ومنع الانجراف الشديد لقاع النهر. يمكن تبديد الطاقة الحركية في حوض التهدئة من خلال تكوين القفزة الهيدروليكية، يمكن تقييم كفاءة حوض التهدئة اعتمادا على خصائص القفزة الهيدروليكية والتي تشمل طول القفزة النسبي، نسبة العمق الثانوي، ومقدار تشتيت الطاقة النسبي. في هذه الدراسة، أجريت اختبارات مختبرية وعددية لتقييم أداء أنواع مختلفة من احواض التهدئة في مؤخر المسيل المائي وباستخدام ستة قيم مختلفة من ارقام فرود تراوحت من ٦٫٣٧ إلى ١٤٫٩٧. أجريت التجارب المختبرية على حوض التهدئة القياسي USBR II واستخدمت النتائج لأجراء تحليل اختبار حجم الشبكة للمحاكاة العددية. تم إجراء عمليات المحاكاة العددية لأحواض التهدئة ذات الأرضية الخشنة باستخدام برنامج FLOW-3D 11.04. تم تصميم ارضيات الحوض الخشنة باستخدام ثلاث نسب مختلفة لتوزيع البلوكات (١٠٪، ١٥٪، ٢٢٪) وثلاثة ارتفاعات نسبية مختلفة (٠٫٥، ٠٫٧٥، ١). أشارت النتائج إلى ان توزيع بلوكات مكعبة الشكل في قاع الحوض بنسبة١٠ ٪ وارتفاع خشونة نسبي يساوي (١) أدى الى زيادة كفاءة الحوض مقارنة بالأرضية الملساء والارضيات الخشنة الاخرى. في الحالة المثلى للقاع الخشن كانت نسبة العمق الثانوي اقل ب ١٢٫١٪ ومقدار تشتيت الطاقة اعلى ب ٥٫١٪ مقارنة بالحوض القياسي.

الكلمات الدالة: القفزة الهيدروليكية، محاكاة عددية، تشتيت الطاقة النسبي، الخشونة، نسبة العمق الثانوي، حوض التهدئة.

1.INTRODUCTION

Hydraulic structures, such as dams, spillways, and weirs, are the most significant engineering structures partially or entirely immersed in water [1]. The high kinetic energy of flow at the outlet of these structures is among the causes of hydraulic and structural failures. When the highly-accelerated water is directly released into the downstream channel, a significant scour may move backwards to the hydraulic structure, endangering it [2]. Therefore, this high kinetic energy of the flow should be dissipated to avoid severe scouring of the downstream riverbed and ensure that water is returned to the river with optimal energy conditions. Hydraulic jump is a traditional energy dissipation mechanism in which the flow rapidly transitions from supercritical to subcritical, causing a sudden rise in the water surface. However, the hydraulic jump creates extremely complex features, including significant air entrainment, turbulence, spray, surface waves, and fluctuations in pressure and velocity. Due to these features, the high energy of the incoming flow is lost, and the water is released to the river with the proper energy conditions [3]. Numerous energy dissipators are available; the most used types are stilling basins, roller buckets, and flip buckets. Despite being more expensive, investigations have shown that the hydraulic jump-type stilling basin is the best among alternative energy dissipators. According to numerous studies, implementing the design criteria developed by the Bureau of Reclamation in the United States (USBR) for designing stilling basins provides superior performance. The most prevalent USBR stilling basins are types I, II, III, and IV, which are classified based on the upstream Froude number. The most effective stilling basin design requires the following hydraulic jump features: a smaller sequent depth ratio, high energy dissipation, and shorter length. To satisfy these requirements, accessories like chute blocks, baffle piers, roughness elements, and sills are installed in the basin with different geometries and arrangements. According to many studies, installing roughness elements in the bed of a stilling basin significantly affects its performance. Mohamed Ali [4] experimentally investigated the effect of roughness length (L_r) on the performance of a stilling basin. For this purpose, cubic elements were distributed in the rectangular flume bed in a staggered-protruded way. The results indicated that utilizing cube roughness resulted in a noticeable reduction in the hydraulic jump's length and enhanced the efficiency of the stilling basin. Ead and Rajaratnam [5] studied the properties of hydraulic jump on the sinusoidal corrugated bed for Froude numbers 4 to 10 and different relative roughness heights. The results showed that the sequent depth ratio was insignificantly affected by the relative roughness, as the corrugation crest was placed at the same elevation as the upstream bed and thus acted as cavities. The tailwater depth and jump length were reduced by 25% and 50%, respectively, compared to the smooth bed. Bejestan and Neisi [6] developed a new roughened bed stilling basin by arranging prismatic lozenge-shaped elements in staggered patterns in the bed of a rectangular flume. The results indicated that the jump's length and the tailwater depth were reduced by about 41% and 26%, respectively, compared to the classical jump. The new stilling basin length was comparable to the USBR II basin when the Froude number ranged from 4.5-7, and it was shorter and nearly identical to the USBR III stilling basin length for Froude numbers more than 7. Parsamehr et al. [7] tasted the effects of an adverse slope and a rough bed on the main features of a hydraulic jump. Observations revealed that the bed shear stress induced by bed roughness decreased the sequent depth ratio and increased energy dissipation by forming large eddies and additional turbulent flow. Several numerical techniques have been developed in the last decade, benefiting from the rapidly increasing computing power and motivation generated by the need to overcome the potential scale effects of laboratory-scale models [8, 9]. However, the Computational Fluid Dynamics (CFD) technique is an advanced tool for simulating flow in hydraulic structures, particularly those where turbulent and aeration effects should considered, such as hydraulic jumps and water jets [10]. This technique provides practitioners with quantitative and qualitative data. FLOW-3D software is the most widely used CFD code in hydraulic engineering applications, and it has been successfully reported in recent studies on energy dissipation, waving, and scouring. Daneshfaraz et al. [11] investigated the impact of roughness blocks on the bed of an ogee spillway using computational fluid dynamics. Several independent parameters were modified, including flip bucket angle, bed roughness, and Froude number. The free-flow surface was modeled using the *RNG k-* turbulence model and the volume of fluid technique. The results demonstrated that the numerical model can accurately predict a free-flow surface over an ogee spillway. Güven and Mahmood [12] used Flow-3D to simulate flow properties, including velocity distribution, air entrainment, and dynamic pressure distribution above a stepped spillway with a sudden slope change. The numerical simulation results were compared to experimental results from the literature. Zaffar and Hassan [13] numerically simulated the hydraulic jump features in different types of stilling basins with wedge-shaped blocks using FLOW-3D. The proposed stilling basin results were compared to the USBR type III basin and literature. According to the reviewed literature, which demonstrated the present understanding of stilling basins, no study has yet evaluated the performance of the Typical USBR II stilling basin using a rough bed. The novel aspect of the present work is adding cubic roughness elements with various intensities and heights to the bed of the USBR II stilling basin and finding the most efficient case. Experimental and numerical runs were performed to achieve the goal of this study.

2.EXPERIMENTAL WORKS

Experiments were conducted in a flume that measured 20 m in working length, 0.6 deep, and 0.9 m in width. The flume was constructed from a steel plate with an armored plate-glass sidewall. The water flow was controlled via a manually operated valve on the circulation system. The main pump can be maintained at a stable operation using a bypass pipe installed on the supply pipe and controlled by a butterfly valve. The discharge measurement was conducted using a 90° v-notch sharp-crested weir installed 3m downstream of the inlet tank. An ogee spillway model was designed according to standard spillway shape (WES), which was developed by the US Army Corps of Engineers-Waterways-Experimental Station (USACE-WES) [14, 15]. The spillway was placed in the middle third of the laboratory flume, 7m upstream of the tailgate, as shown in Fig. 1. The tailgate was placed at the downstream end of the flume to adjust and control the tailwater depth, ensuring that the jump occurred at the downstream end of the spillway (toe). A Typified USBR II stilling basin was designed according to the maximum applied discharge (33 ℓ/s), as illustrated in Fig. 2. The energy dissipation accessories, i.e., chute blocks and end sill, were fabricated using a Creality Ender 3 V2 3D printer with Polylactic Acid (PLA), which is one of the most prevalent thermoplastics. The fabricated accessories were then fixed to the stilling basin bed using Soma Fix S665 glue. Experiments were conducted under six upstream Froude numbers: 6.37, 7.28, 8.16, 9.45, 11.62, and 14.97, which corresponded to discharges of 33, 28, 23, 18, 13, and 8 ℓ/s, respectively. In each test, the flume was adjusted to a horizontal position, and the tailgate was progressively adjusted to capture the jump within the stilling basin with its toe near the downstream end of the spillway model. The initial depth of the hydraulic jump was measured at least three times along the upstream cross-section with a digital vernier, and the average value was calculated. Similarly, more than two measurements for sequent depth were recorded using a point gauge along the downstream cross-section, and the average value was considered, as shown in Fig. 1.

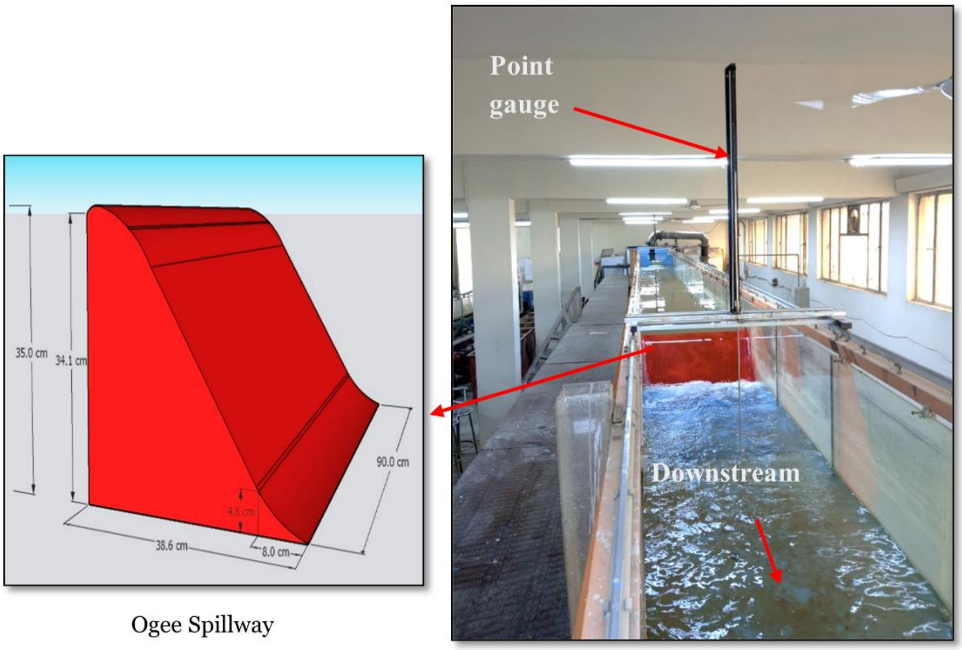

Fig. 1 Ogee Spillway Installed in the Laboratory Flume.

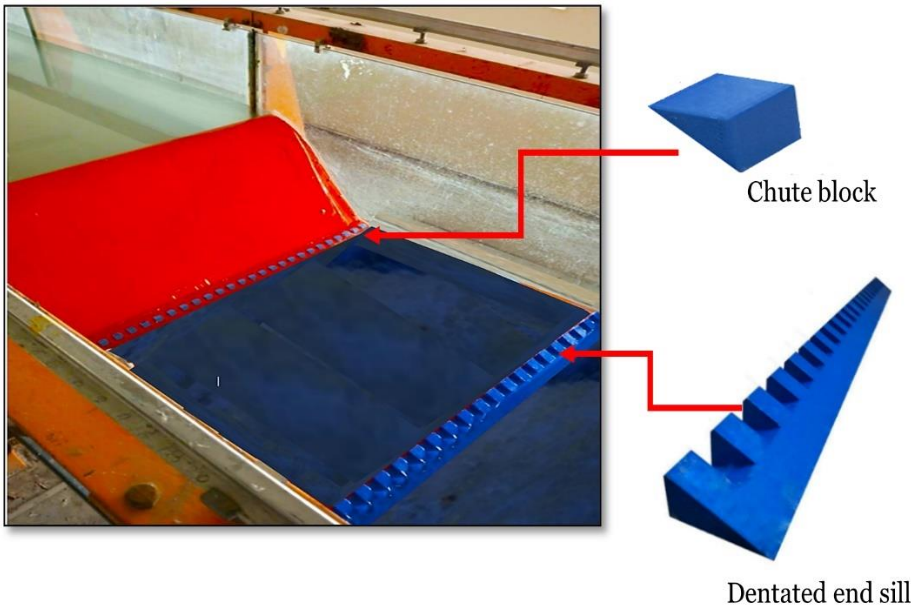

Fig. 2 A Physical Model of the Typical USBR II Stilling Basin.

3.NUMERICAL SIMULATION

In the present study, numerical simulations were performed for the USBR II stilling basin with different rough beds instead of smooth beds. The following stages provide a brief description of the essential processes considered in developing numerical models:

3.1.Model Geometry and Mesh Generation

The geometry of any numerical model was created using Sketch-Up Pro 2022 software. Then, the sketched model was exported to FLOW-3D as a stereolithography file format (STL). The exported geometry files included the Ogee spillway model and the proposed stilling basin. The second essential stage in preprocessing was meshing, or grid generation, which defined all considered structures and free space zones. The computational domain was meshed with two structured rectangular hexahedral blocks: containing and nested. A contained mesh block was constructed for the entire spatial domain, which includes the spillway and the stilling basin. A nested mesh block of refined cells was created for the region of interest, which involves the end of the ogee spillway and the entire stilling basin area where the hydraulic jump occurs. The equations governing fluid motion fall into the category of initial-boundary condition problems. Therefore, the solution must be known initially and at the boundaries to solve the governing equations inside the domain. In this study, six boundary conditions for each mesh block were applied based on the experimental conditions, as shown in Fig. 3. For a containing mesh block, the inlet boundary condition was defined as a discharge value corresponding to the water elevation upstream of the spillway. On the other hand, the downstream end of the domain was defined as a pressure boundary condition in terms of the tailwater elevation. The bottom and sides of the containing block domain were set to a wall no-slip boundary condition, while an atmospheric pressure ($P = 0$) was used for the upper boundary condition. The symmetric boundary conditions were applied to the intermediate borders between two mesh blocks. A fluid region with a corresponding elevation was defined upstream of the ogee spillway for the initial condition.

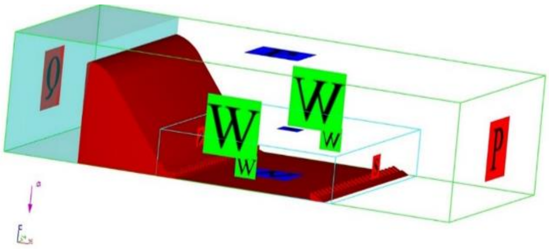

Fig. 3 Boundary Conditions Used in the Numerical Simulation.

3.2.Turbulence Modelling

This study implemented the numerical simulation of two-phase flow involving hydraulic jump using FLOW-3D software that uses the finite volume method for solving the Reynolds average Navier–Stokes equations (RANS) [16]. Averaging Navier–Stokes equations introduce Reynolds stresses into the simulation and add new terms involving turbulent viscosity. This averaging results in the turbulence closure problem in the governing equations of flow, which can be solved using an appropriate turbulence model. In the Flow-3D program, three types of two-equation turbulence transport models are incorporated, including the standard $(k-\varepsilon)$, Re-Normalization Group $(RNG)(k-\varepsilon)$, and $(k-\omega)$ models. The standard $(k-\varepsilon)$ is the most widespread model, and it performed well for a wide range of turbulent flow models [17]. This model contains two additional transport equations: the first for the turbulent kinetic energy and the second for its dissipation rate. Solving these equations yields the turbulent model's two parameters (k and ε). Then, turbulent eddy viscosity can be calculated using the following formula:

$$\boldsymbol{v_t = c_m \frac{k^2}{\varepsilon}} \qquad \textbf{(1)}$$

where v_t is the turbulent kinematic viscosity, k is turbulent kinetic energy, ε dissipation rate, and c_m is a constant. The $k-\omega$ model usually outperforms the other models and gives reliable estimations in particular flow situations, such as flow near wall borders or with streamwise pressure gradients like wakes and jets. The Re-Normalization Group (RNG) model improves on the $(k-\varepsilon)$ model by accounting for the small-scale effects caused by large-scale motion and by modifying viscosity terms [18]. This modification makes the RNG model accurate enough to simulate hydraulic engineering problems with complex geometry and flow fields, such as flow over spillways and within the stilling basins [11, 19].

3.3.Air Entrainment

Additional physical models for air entrainment must be considered for conditions where aeration forms a significant feature that affects the flow behavior, such as in the hydraulic jump. FLOW-3D computes the rate at which air is entrained into the flow by balancing stabilizing and destabilizing forces [20]. Density evaluation and drift flux models are also used to simulate non-uniform density and air bubble motion, respectively [21]. In the density evaluation model, the fluid was a mixture of two components, each of a constant density, and the weighted average density in each cell was assumed to relate linearly with the two fluid densities, as follows:

$$\boldsymbol{\bar{\rho} = F\rho + (1-F)\rho_a} \qquad \textbf{(2)}$$

where $\bar{\rho}$ is the volume weighted-average density, F is the volume fraction, ρ is the water density, and ρ_a is the air density. The drift flux model considers the interaction between the continuous phase (water) and the dispersed phase (air). The velocity differences occur due to the differences in density between the two phases, resulting in non-uniform body forces [22]. To develop the drift flux model in this study, the minimum and maximum volume fraction (F) values were chosen as 0.1 and 1, respectively. The air density (ρ_a) was set to 1.225 kg/m^3, whereas the density of water (ρ) was set to 1000 kg/m^3 based on the laboratory conditions.

3.4.Mesh Sensitivity

Mesh sensitivity is the most important aspect when selecting the mesh size for numerical modeling. Mesh refinement, i.e., gradually refining the mesh size and grid spacing for the same computational domain, results in more nodes and elements. As a result, the numerical model increases in size and requires more computational time despite producing better results [20]. This study used experimental results for a Typified USBR II stilling basin to analyze sensitivity using five cell sizes. In each test, the cell size of nested blocks was half that of the containing block. Thus, mesh sensitivity was performed under five contained-nested cell sizes: 12-6 mm, 10-5 mm, 8-4 mm, 6-3 mm, and 5-2.5 mm. The sequent depth ratios were calculated and compared to the experimental results during each mesh testing. This procedure was repeated for six Froude numbers. The results are depicted in Fig. 4. It is clear from this figure that the simulated sequent depth ratio exhibited better agreement with that in the experimental model when the cell sizes of containing and nested blocks were 5 mm and 2.5 mm, respectively, with an average relative error of about 5%. However, further mesh refinement may result in an undesirable increase in computational time. Due to computational power limitations, increasing the number of mesh elements in the computational domain may not always be practicable; furthermore, in contrast to the theory that the finer the mesh resolution, the higher the accuracy, using coarser mesh may still provide accurate results. Therefore, to ensure computation efficiency, a 5-2.5 mm cell size grid was adopted in this study to perform a series of simulations, as shown in Fig. 5.

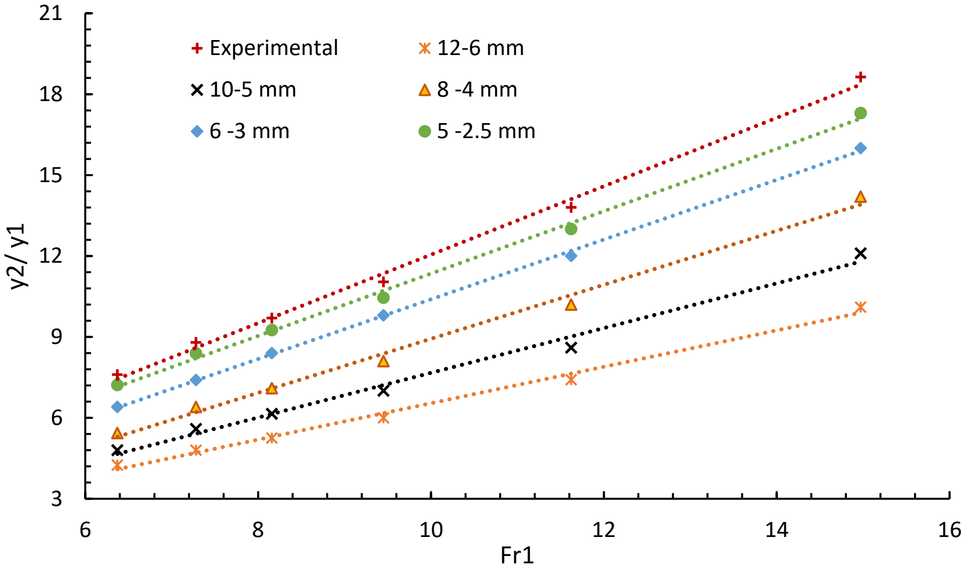

Fig. 4 Mesh Sensitivity Test for the Typified USBR II Model.

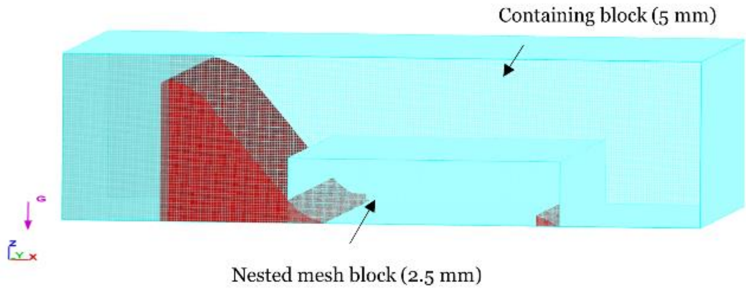

Fig. 5 Computational Domain of Typified USBR II Model with Mesh Sizes 2.5.

3.5.Parameters Affecting the Performance of the Rough Bed Stilling Basin

The USBR II stilling basin with different rough beds was numerically investigated in this study using FLOW – 3D software. Cubic-shaped elements of height h_c, width w_c, and length l_c were installed in the bed of the stilling basin in a staggered pattern. To avoid cavitation, the crests of elements were set at the same level as the upstream bed on which the ogee spillway produced the supercritical flow. Before performing numerical simulations for the rough bed stilling basin, it is necessary to identify the key parameters influencing the features of hydraulic jump formed in the USBR II stilling basin with the prismatic roughness elements, which are as follows:

$$f\left(I, h_c, l_c, w_c\ y_1, y_2, v_1, g, \rho, \mu\right) = 0 \qquad (3)$$

where I is the percent intensity of elements in the bed (dimensionless), which is calculated by dividing the projected area of the elements by the entire area of the roughness-covered basin, h_c is the height of the element (L), l_c is the length of the element, w_c is the width of element (L), y_1 is initial jump depth (L), y_2 is the sequent depth, v_1 is the flow velocity at depth y_1 (L/T), g is the gravitational acceleration (L/T^{-2}), ρ is the mass density of water (M/L^{-3}), and μ is the viscosity of water (ML^{-1}T^{-1}). Using Buckingham's theory, the dimensionless relationship can be expressed as follows:

$$f\left(I, \frac{h_c}{y_1}, \frac{l_c}{y_1}, \frac{w_c}{y_1}\ \frac{y_2}{y_1}, Fr_1, Re\right) = 0 \qquad (4)$$

where Fr_1 is the Froude number of supercritical flow (dimensionless), $\frac{h_c}{y_1}$ relative roughness height, and Re is the Reynolds number of supercritical flow (dimensionless). Due to the hydraulic jump's high turbulence, Reynolds number effects can be ignored [23, 24]. The length and width of elements in this study were kept constant; therefore, the parameters $\frac{l_c}{y_1}$ and

$\frac{w_c}{y_1}$ were eliminated. Thus, Eq. (4) can be rewritten as follows:

$$\frac{y_2}{y_1} = f\left(I, \frac{h_c}{y_1}, Fr_1\right) \quad \textbf{(5)}$$

According to the above formula, the effects of intensity and relative roughness height on the sequent depth ratio and energy dissipation were numerically investigated under six values of the initial Froude number.

3.6.The Geometries of USBR II Stilling Basin with Rough Beds

Numerical models of the stilling basins were developed using three intensities (10%, 15%, and 22%) and three relative roughness heights (1, 0.75, and 0.5). The length and width of the elements were kept constant, i.e., 1.5 cm, in all tests, equivalent to the initial depth corresponding to the design discharge. For a stilling basin with a roughness intensity of 10%, the elements were arranged in the bed in a staggered pattern. The transverse and longitudinal distance between any two adjacent elements was $2y_1$. Additionally, the first row of roughness elements began at a distance $2y_1$ downstream of the spillway, as shown in Fig. 6, where y_1 is the initial depth corresponding to the design discharge. The stilling basin with a roughness intensity of 15 % was designed so that the transverse and longitudinal distance between two adjacent elements was $1.5y_1$. The roughness began at a distance $1.5y_1$ downstream of the spillway, as shown in Fig. 7. To increase the intensity of roughness to 22%, the transverse and longitudinal distances between two adjacent elements were reduced to be equal to y_1, and the roughness began at distance y_1 downstream of the spillway, as shown in Fig. 8. All three models have the same relative roughness height (1). Each model was numerically simulated under the Froude number range of 6.37–14.97. In each run, the tailwater depth, i.e., downstream boundary condition, was adjusted so that the jump began at the entrance of the stilling basin. The stilling basin with the most efficient intensity was chosen to be numerically tested with two relative roughness heights of 0.75 and 0.5, i.e., h_c =1.125 and 0.75 cm.

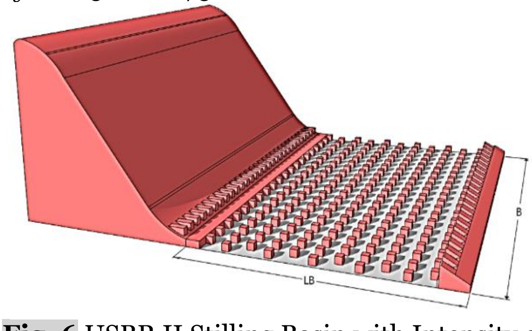

Fig. 6 USBR II Stilling Basin with Intensity of 10% And Relative Roughness Height (1).

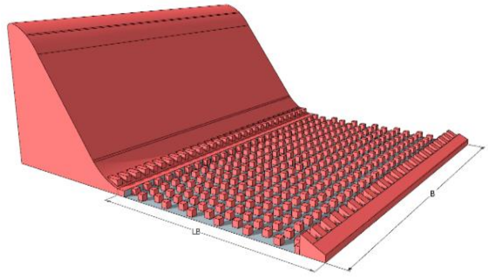

Fig. 7 USBR II Stilling Basin with Intensity of 15% and Relative Roughness Height (1).

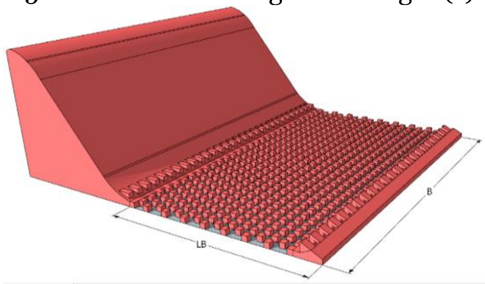

Fig. 8 USBR II Stilling Basin with Intensity of 22% and Relative Roughness Height (1).

4.RESULTS AND DISCUSSION

4.1.Roughness Intensity

The sequent depth ratio values are plotted versus the inflow Froude number for three intensities, together with a Typified stilling basin, as shown in Fig. 9. The figure shows that the intensity of artificial bed roughness significantly impacted the sequent depth, decreased with (I), reaching a minimum value at I=10%. Additionally, the value of (y_2/y_1) increased with the initial Froude number (Fr_1) values for the same intensity (I). The average reduction values in sequent depth ratio compared to the Typified stilling basin were 12.2%, 10.1%, and 5% for I =10%, 15%, and 22%, respectively. Additionally, the relative energy loss was high at I= 10% for six values of the initial Froude number, as shown in Fig. 10. The average gains in energy dissipation were 5.1%, 4.2%, and 1.6% for I =10%, 15%, and 22%, respectively. Figures 11 to 13 illustrate the flow depth and velocity vector simulations for stilling basins with roughness intensities of 22%, 15%, and 10%, respectively. These figures indicate that the lower tailwater depth was achieved for the same hydraulic conditions when the roughness intensity was 10%. Thus, utilizing a rough bed instead of a smooth bed enhanced the efficiency of the USBR II stilling basin, which may be attributed to the interaction between supercritical flow and the roughness elements, which created a system of turbulent eddies and increased the bed shear stresses. The turbulence level decreased with increasing (I) due to the close spacing between elements, behaving as a smooth bed. These findings confirmed the previous studies regarding the intensity of roughness elements, which stated that the most efficient intensity for rectangular staggered elements was 10% [4, 5].

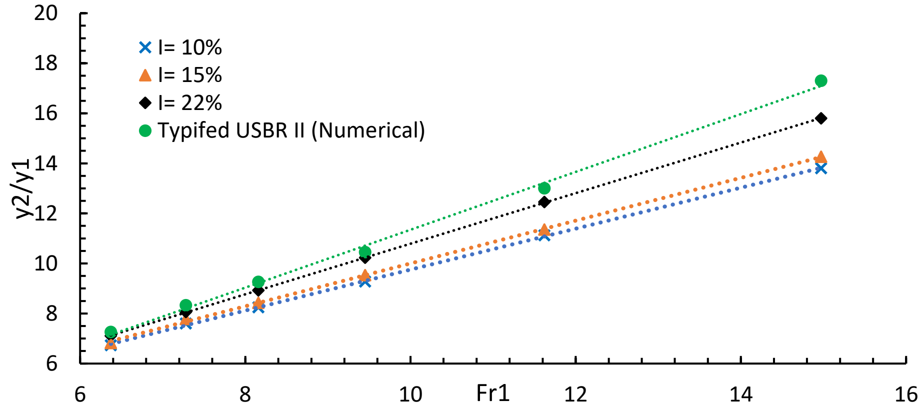

Fig. 9 Sequent Depth Ratio for USBR II Stilling Basin at Different Roughness Intensities.

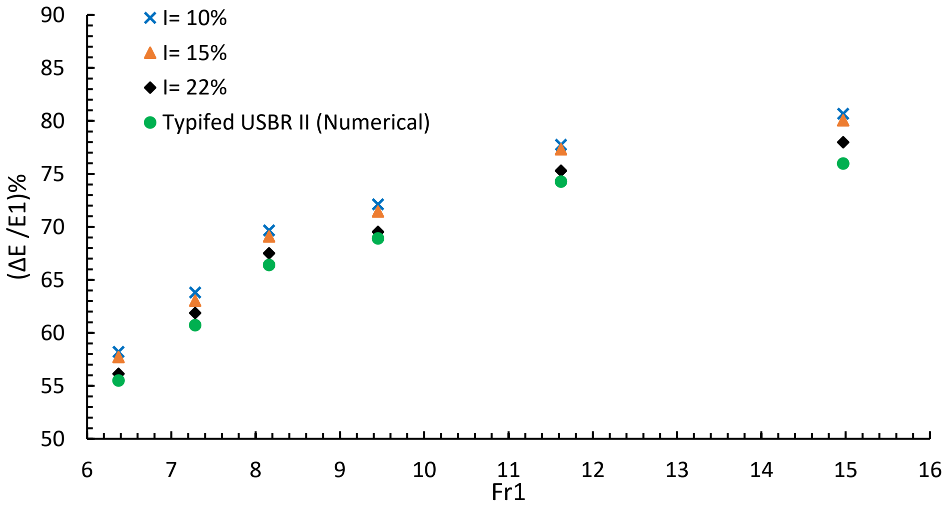

Fig. 10 Relative Energy Loss for USBR II Stilling Basin at Different Roughness Intensities.

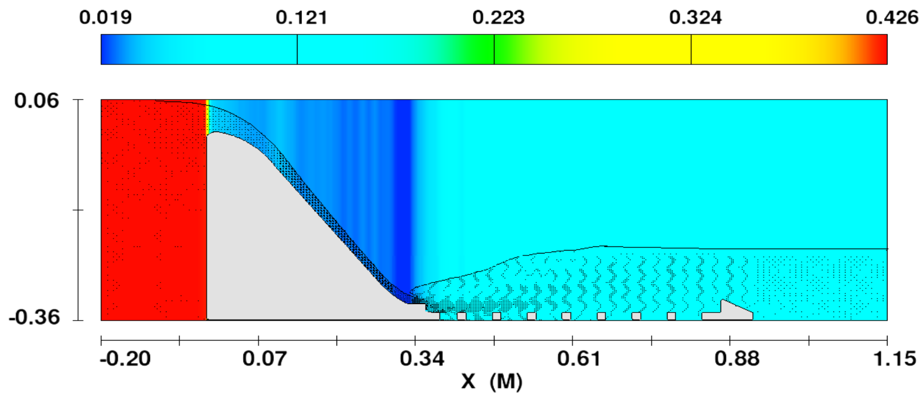

Fig. 11 Flow Depth and Velocity Vector for USBR II Stilling Basin at I= 22% and Fr_1=6.37.

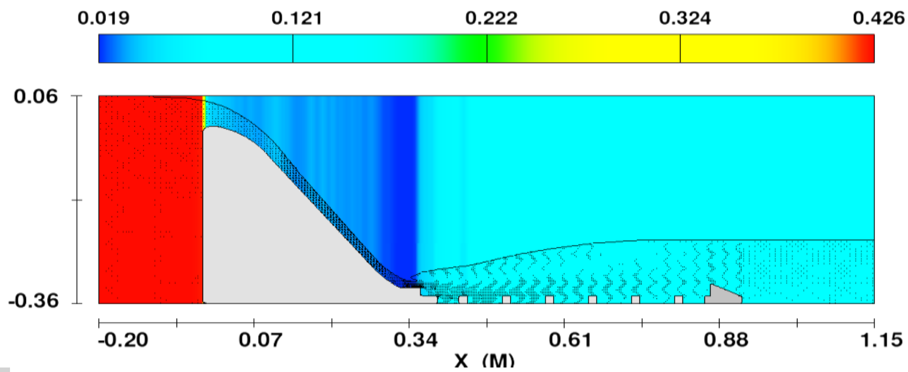

Fig. 12 Flow Depth and Velocity Vector for USBR II Stilling Basin at I= 15% and Fr_1=6.37.

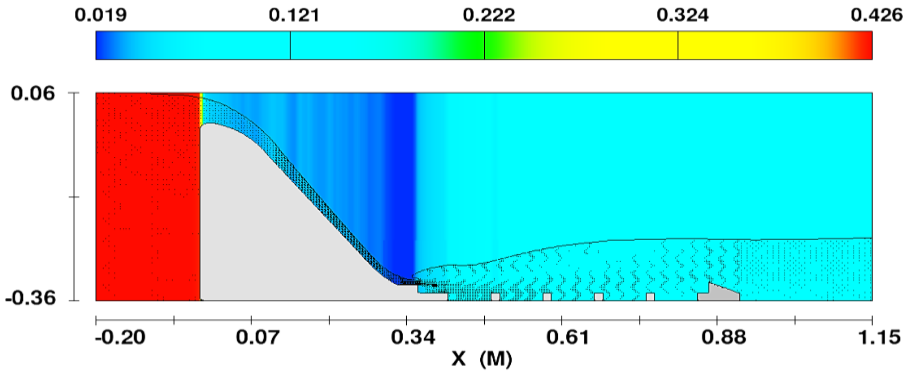

Fig. 13 Flow Depth and Velocity Vector for USBR II Stilling Basin at I= 10% and Fr_1=6.37.

4.2.Relative Roughness Height

To investigate the effect of the relative roughness parameter (h_c/y_1) on the characteristics of the hydraulic jump formed in the USBR II stilling basin, staggered roughness elements were arranged in the bed with un optimum intensity of 10%. Then, numerical tests were performed under three relative roughness values: 0.5, 0.75, and 1. The numerical simulation results indicated that the tailwater required for a stilling basin with a rough bed was lower than for a smooth bed due to recirculation vortex and flow separation between the roughness elements. As shown in Figs. 14 and 15, the variations in sequent depth ratio and energy dissipation depended on the initial Froude number and the relative roughness height. Increasing the height of the dissipative elements reduced the sequent depth ratio and enhanced energy dissipation, respectively. Compared to the Typified stilling basin, the average reduction in the sequent depth ratios was about 12.1%, 8%, and 5.7% for relative roughness values 1, 0.75, and 0.5, respectively. On the other hand, the average gains in energy dissipation were 5.1%, 3.3%, and 2.3% for relative roughness values 1, 0.75, and 0.5, respectively. Figures 16 to 18 show the turbulence intensity simulations in stilling basins with relative roughness heights of 1, 0.75, and 0.5, respectively. According to these figures, the turbulence intensity was high at the entrance section of the stilling basin near the chute blocks due to the creation of vortices. Approaching the end of the stilling basin, the turbulence intensity tends to decrease and become more uniform. These figures also show that the turbulence intensity in the bed with a relative roughness of (1) decreased and became uniform at a short distance from the inlet section compared to the beds with relative roughness of 0.75 and 0.5. According to previous studies, relative roughness up to (1) was recommended for designing rough beds, although increasing this parameter causes more turbulence and flow separation; however, it may be inefficient from practical and economical viewpoints.

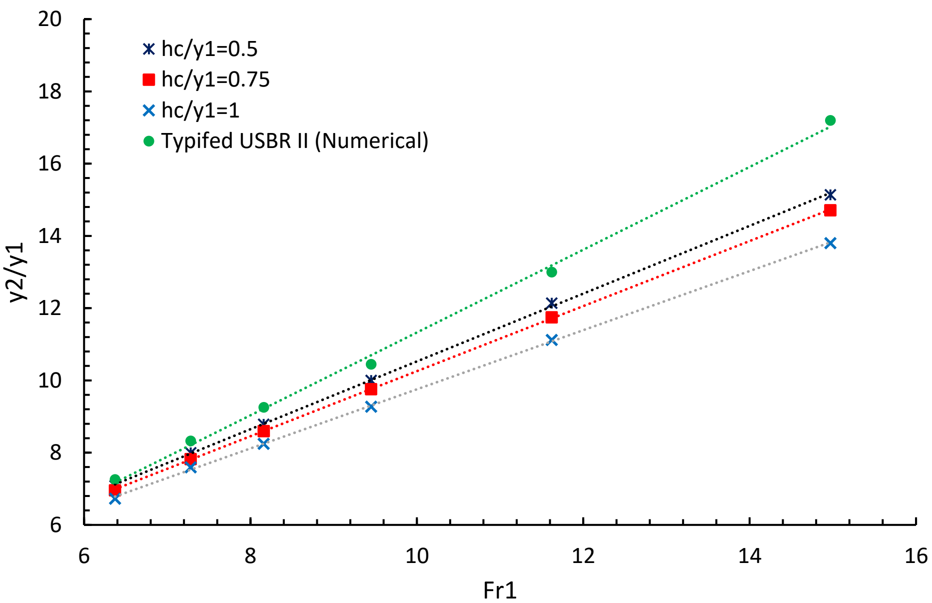

Fig.14 Sequent Depth Ratio for USBR II Stilling Basin at I=10% and Different Relative Roughness Heights.

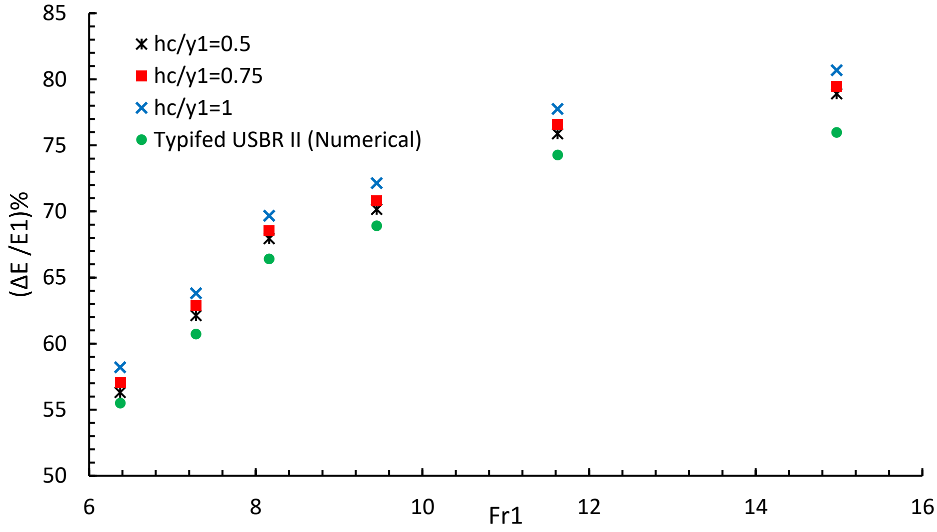

Fig.15 Relative Energy Loss for USBR II Stilling Basin at I=10% and Different Relative Roughness Heights.

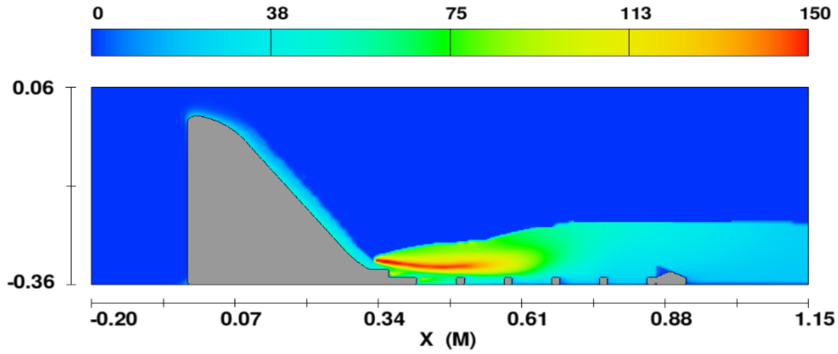

Fig. 16 Turbulence Intensity Contours in USBR II Stilling Basin: $\boldsymbol{Fr_1}$=6.37, I=10%, and $\boldsymbol{h_c/y_1 = 1}$.

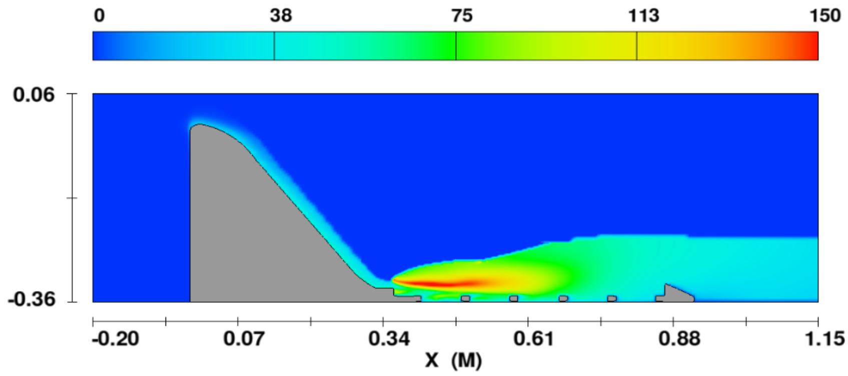

Fig. 17 Turbulence Intensity Contours in USBR II Stilling Basin: $\boldsymbol{Fr_1}$=6.37, I=10%, and $\boldsymbol{h_c/y_1 = 0.75}$.

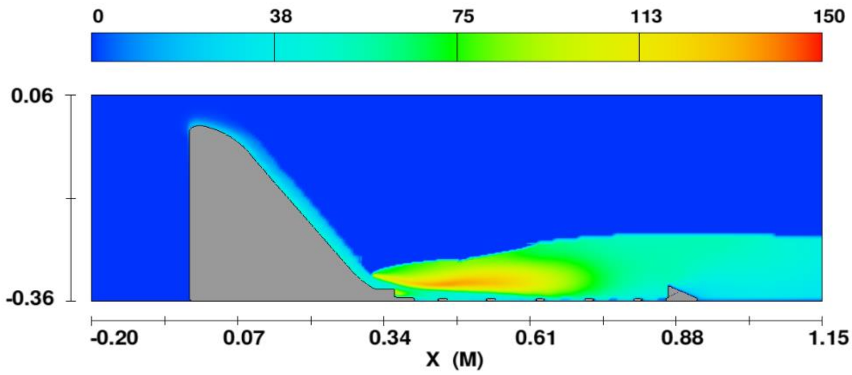

Fig.18 Turbulence Intensity Contours in USBR II Stilling Basin: $\boldsymbol{Fr_1}$=6.37, I=10%, and $\boldsymbol{h_c/y_1 = 0.5}$.

5.CONCLUSIONS

A Typified USBR II stilling basin was modified in this study to achieve a more efficient basin downstream of the ogee spillway using experimental and numerical modeling. Modification processes involved using five rough beds instead of a smooth bed. The following are the main conclusions of the present study:

- The verification results indicated a satisfactory agreement between the numerical and experimental sequent depth ratios, where the average relative error was 5%.
- According to the numerical simulations, distributing cubic roughness elements in the bed of the USBR II stilling basin in a staggered way enhanced the performance of the stilling basin compared to the typified basin.
- The USBR II stilling basin with roughness elements distributed at an intensity of 10% performed better than those with beds of intensity of 15% and 22%. Due to the close spacing between elements, which behaved like a smooth bed, turbulence decreased as intensity increased.
- Increasing the height of roughness caused more turbulence and flow separation. Roughness elements of relative height (1) and 10% intensity were more effective in the USBR II stilling basin than those of relative heights (0.75 and 0.5) and at the same intensity (10%).
- Compared to the typified basin, distributing staggered roughness elements in the bed of the USBR II stilling basin at 10% intensity and a relative roughness height of (1) decreased the sequent depth ratio by 12.1% and enhanced energy dissipation by 5.1%.

ACKNOWLEDGEMENTS

The authors are grateful to the Civil Engineering Department at Basrah University for supporting this research. Postgraduate Research Grant (PGRG) No.3/13/14264 (28/10/2020).

NOMENCLATURE

E_1	Specific energy at the upstream section of the hydraulic jump, m
F	Air volume fraction
Fr_1	Froude number of incoming flow
g	Gravitational acceleration, m/s^2
h_c	Height of roughness element, m
I	Percent intensity
k	Turbulent kinetic energy, m^2/s^2
l_c	Length of roughness element, m
L_r	Roughness length, m
Q	Discharge, ℓ/s
Re	Reynolds number
v_1	Velocity at the upstream section of the hydraulic jump, m/s
w_c	Width of roughness element, m
y_1	Initial depth, m
y_2	Sequent depth, m
y_1/y_2	Sequent depth ratio
Greek symbols	
ε	Dissipation rate, m^2/s^3
μ	Dynamic viscosity, kg/ (m s)
v_t	Turbulent kinematic viscosity, m^2/s
ρ	Mass density of water, kg/m^3
ρ_a	Mass density of air, kg/m^3
$\bar{\rho}$	Volume- weighted average density, kg/m^3

REFERENCES

[1] Saleh LA, Khassaf SI, Abeed KR. **Predicting the Breach Hydrograph Resulting Due to Hypothetical Failure of Haditha Dam**. *Jordan Journal of Civil Engineering* 2011; **5**(3): 392–400.

[2] Rashak BM, Khassaf SI. **Local Scour Around T-Shape Submerged Groynes in Clear Water Conditions.** *International Journal of GEOMATE* 2021; **20**(77): 163–172.

[3] Chow VT. ***Open Channel Hydraulic***. 1st ed., New York: McGraw-Hill;1959.

[4] Mohamed Ali HS. **Effect of Roughened-Bed Stilling Basin on Length of Rectangular Hydraulic Jump**. *Journal of Hydraulic Engineering* 1991; **117**(1): 83–93.

[5] Ead SA, Rajaratnam N. **Hydraulic Jumps on Corrugated Beds**. *Journal of Hydraulic Engineering* 2002; **128**(7): 656–663.

[6] Bejestan MS, Neisi K. **A New Roughened Bed Hydraulic Jump Stilling Basin**. *Asian Journal of Applied Sciences* 2009; **2**(5): 436–445.

[7] Parsamehr P, Kuriqi A, Farsadizadeh D, Dalir AH, Daneshfaraz R, Ferreira RM. **Hydraulic Jump Over an Adverse Slope Controlled by Different Roughness Elements**. *Water Resources Management* 2022; **36**(14): 5729–5749.

[8] Mohammed Saleh LA, Majeed SA, Alnasrawi FA. **Numerical Study of the Bridge Pier Scour Using Gene Expression Programming**. *Journal of Applied Water Engineering and Research* 2019; 7(4): 287–294.

[9] Mohammed Saleh LA, Khassaf SI, Al-Murshidi KR. **Application HEC-RAS Model to Simulate the Flood Wave Due to Dam Failure**. *4th Scientific International Conference Najaf (SICN)* 2019; Najaf, Iraq. p. 150–155.

[10] Irzooki RH, Mohammed JR, Ameen AS. **Computational Fluid Dynamics Modeling of Flow Over Stepped Spillway**. *Tikrit Journal of Engineering Sciences* 2016; **23**(3): 1–11.

[11] Daneshfaraz R, Ghaderi A, Akhtari A, Di Francesco S. **On the Effect of Block Roughness in Ogee Spillways with Flip Buckets**. *Fluids* 2020; **5**(4): 182, (1-17).

[12] Güven A, Mahmood AH. **Numerical Investigation of Flow Characteristics Over Stepped**

Spillways. *Water Supply* 2021; **21**(3): 1344–1355.
[13] Zaffar MW, Hassan I. **Numerical Investigation of Hydraulic Jump for Different Stilling Basins Using FLOW-3D**. *AQUA Water Infrastructure, Ecosystems and Society* 2023; **72**(7): 1320–1343.
[14] Uncan W, Hokenstrom J, Huntley C, Cudworth A, McDaniel T. **Design of Small Dams**. United States: A Water Resources Technical Publication; 1987 .
[15] Khatsuria RM. **Hydraulics of Spillways and Energy Dissipators**. 1st ed., CRC press; 2004.
[16] Versteeg HK, Malalasekera W. **An Introduction to Computational Fluid Dynamics: the Finite Volume Method**. 1st ed., England: Longman; 1995.
[17] Rodi W. **Turbulence Models and their Application in Hydraulics**. 1st ed., London: Routledge; 1993.
[18] Yakhot V, Orszag SA, Thangam S, Gatski TB, Speziale CG. **Development of Turbulence Models for Shear Flows by a Double Expansion Technique**. *Physics of Fluids A: Fluid Dynamics* 1992; **4**(7): 1510–1520.
[19] Li S, Zhang J. **Numerical Investigation on the Hydraulic Properties of the Skimming Flow Over Pooled Stepped Spillway**. *Water* 2018; **10**(10): 1478, (1-19).
[20] Dong Z, Wang J, Vetsch D, Boes RM, Tan G. **Numerical Simulation of air-Water Two-Phase Flow on Stepped Spillways Behind X-Shaped Flaring Gate Piers under Very High Unit Discharge**. *Water* 2019; **11**(10): 1956, (-21).
[21] Flow Science Inc. FLOW-3D Version 11.0.4 - User Manual. United States; 2015.
[22] Macián-Pérez JF, García-Bartual R, Huber B, Bayon A, Vallés-Morán FJ. **Analysis of the Flow in a Typified USBR II Stilling Basin Through a Numerical and Physical Modeling Approach**. *Water* 2020; **12**(1): 227, (1-20).
[23] Dasineh M, Ghaderi A, Bagherzadeh M, Ahmadi M, Kuriqi A. **Prediction of Hydraulic Jumps on a Triangular Bed Roughness Using Numerical Modeling and Soft Computing Methods**. *Mathematics* 2021; **9**(23): 3135, (1-24).
[24] Parsamehr P, Farsadizadeh D, Hosseinzadeh Dalir A, Abbaspour A, Nasr Esfahani MJ. **Characteristics of Hydraulic Jump on Rough Bed with Adverse Slope**. *ISH Journal of Hydraulic Engineering* 2017; **23**(3): 301–307.